



A Theoretical Study of CoCN in the $^3\Phi$ Electronic Ground State

Tsuneo Hirano, Rei Okuda, Umpei Nagashima, Per Jensen

► To cite this version:

Tsuneo Hirano, Rei Okuda, Umpei Nagashima, Per Jensen. A Theoretical Study of CoCN in the $^3\Phi$ Electronic Ground State. *Molecular Physics*, 2007, 105 (05-07), pp.599-611. 10.1080/00268970601126734 . hal-00513065

HAL Id: hal-00513065

<https://hal.science/hal-00513065>

Submitted on 1 Sep 2010

HAL is a multi-disciplinary open access archive for the deposit and dissemination of scientific research documents, whether they are published or not. The documents may come from teaching and research institutions in France or abroad, or from public or private research centers.

L'archive ouverte pluridisciplinaire **HAL**, est destinée au dépôt et à la diffusion de documents scientifiques de niveau recherche, publiés ou non, émanant des établissements d'enseignement et de recherche français ou étrangers, des laboratoires publics ou privés.



A Theoretical Study of CoCN in the $\Lambda^3 \Sigma^-, \Phi$ Electronic Ground State

Journal:	<i>Molecular Physics</i>
Manuscript ID:	TMPh-2006-0038.R1
Manuscript Type:	Full Paper
Date Submitted by the Author:	25-Oct-2006
Complete List of Authors:	Hirano, Tsuneo; Ochanomizu University Okuda, Rei; National Institute of Advanced Industrial Science and Technology Nagashima, Umpei; National Institute of Advanced Industrial Science and Technology Jensen, Per; Bergische Universität Wuppertal, FB C Theoretical Chemistry
Keywords:	ab initio, $\Lambda^3 \Sigma^-, \Phi$ CoCN, structure, rotation-vibration spectrum
Note: The following files were submitted by the author for peer review, but cannot be converted to PDF. You must view these files (e.g. movies) online.	
Hirano_CoCN_revised_3.tex	

A Theoretical Study of CoCN in the $^3\Phi$ Electronic Ground State

TSUNEO HIRANO*

Department of Chemistry, Faculty of Science, Ochanomizu University, 2-1-1 Otsuka,
Bunkyo-ku, Tokyo 112-8610, Japan

REI OKUDA and UMPEI NAGASHIMA

Research Institute for Computational Sciences, National Institute of Advanced Industrial Science and Technology,
1-1-1 Umezono, Tsukuba, Ibaraki 305-8568, Japan

PER JENSEN†

Theoretische Chemie, Bergische Universität, D-42097 Wuppertal, Germany

(Received 00 Month 200x; In final form 00 Month 200x)

We report here *ab initio* calculations of three-dimensional potential energy surfaces for CoCN in its electronic ground state $\tilde{X}^3\Phi_i$ at the MR-SDCI+Q+ E_{rel} /[Roos ANO (Co), aug-cc-pVQZ (C,N)] level of theory. Molecular constants for Co¹²CN and Co¹³CN have been derived by second-order perturbation theory, and rotation-vibration energies have been obtained by the variational MORBID method. At equilibrium, $^3\Phi_i$ CoCN is linear with $r_e(\text{Co-C}) = 1.8540 \text{ \AA}$ and $r_e(\text{C-N}) = 1.1677 \text{ \AA}$. The zero-point averaged structure, however, is bent; the average bond angle is $\langle\angle(\text{Co-C-N})\rangle_0 = 172^\circ$ and the average bond lengths are $\langle r(\text{Co-C})\rangle_0 = 1.8733 \text{ \AA}$ and $\langle r(\text{C-N})\rangle_0 = 1.1718 \text{ \AA}$. Sheridan *et al.* [P. M. Sheridan, M. A. Flory, and L. M. Ziurys. *J. Chem. Phys.*, **121**, 8360 (2004)] have determined from the pure rotational spectrum that $r_0(\text{C-N}) = 1.1313(10) \text{ \AA}$ for $^3\Phi_i$ CoCN; this value is significantly shorter (by about 3.5%) than the *ab initio* value of $\langle r(\text{C-N})\rangle_0$. In contrast, our theoretical value for the rotational constant $B_{0,\Omega=4}$ differs only 0.7% from the experimental value. As discussed previously for $^6\Delta_i$ FeNC [T. Hirano, R. Okuda, U. Nagashima, V. Špirko, and P. Jensen. *J. Mol. Spectrosc.*, **236**, 234 (2006)], the poor agreement between theory and experiment for the C-N bond length is caused by an inadequate treatment of the large-amplitude bending motion of $\tilde{X}^3\Phi_i$ CoCN in the experimental r_0 determination.

1 INTRODUCTION

In a recent paper on $^6\Delta_i$ FeNC [1], we carried out *ab initio* calculations at the MR-SDCI+Q+ E_{rel} /[Roos ANO (Fe), aug-cc-pVQZ (C, N)] level of theory and determined the equilibrium N-C bond length of $^6\Delta_i$ FeNC, $r_e(\text{N-C})$, to be 1.1823 \AA . This value was compared to the value of $r_0(\text{N-C}) = 1.03(8) \text{ \AA}$ determined for $\tilde{X}^6\Delta$ FeNC in 2001 by Lie and Dagdigian [2] from values of the rotational constants B_0 for FeN¹²C and FeN¹³C; the B_0 values were obtained from analysis of the $^6\Pi_{\Omega=7/2} \leftarrow ^6\Delta_{\Omega=9/2}$ electronic transition observed in near-UV laser fluorescence experiments. The experimentally derived r_0 -value is very much shorter than the *ab initio* r_e -value. Also, the $r_0(\text{N-C})$ -value lies outside the range of $1.16\text{--}1.19 \text{ \AA}$ that chemical experience suggests for a typical C-N bond. The B_0 -values used by Lie and Dagdigian [2] to determine the $r_0(\text{N-C})$ -value of $^6\Delta_i$ FeNC were determined from electronic spectra, and so their uncertainties are large compared to those of B_0 -values from rotational spectra. Consequently, the uncertainty $\sigma = 0.08 \text{ \AA}$ given by Lie and Dagdigian [2] for their r_0 -value is rather large [2, 3] compared to typical uncertainties of r_0 -values determined from rotational spectra. However, even with this large uncertainty, the 1σ -interval of $(1.03 \pm 0.08) \text{ \AA}$ does not overlap with the $1.16\text{--}1.19 \text{ \AA}$ interval suggested

*Present address: Research Institute for Computational Sciences, National Institute of Advanced Industrial Science and Technology, 1-1-1 Umezono, Tsukuba, Ibaraki 305-8568, Japan; E-mail: hirano@nccsk.com

†Corresponding author. Tel: +49 202 439 2468; Fax: +49 202 439 2509; E-mail: jensen@uni-wuppertal.de

by chemical experience (whereas the 2σ -interval obviously does overlap). We showed in Ref. [1] that the extraordinarily short $r_0(\text{C-N})$ -value is caused by the neglect of the large-amplitude bending motion of FeNC when the r_0 -value is calculated from the B_0 -values. A more physically meaningful measure of the NC bond length in ${}^6\Delta_i$ FeNC is the expectation value $\langle r(\text{N-C}) \rangle_0 = 1.1866$ Å computed in the variational MORBID calculations [4–7] that are based on the *ab initio* potential energy surface.

For $\tilde{X}^3\Phi_i$ CoCN, Sheridan *et al.* [8] obtained $r_0(\text{C-N}) = 1.1313(10)$ Å from the B_0 values (determined by analysis of pure rotational spectra) for Co^{12}CN and Co^{13}CN . Again, this $r_0(\text{C-N})$ -value is outside the expected range of 1.16–1.19 Å, but it is not so very short as in the case of $\tilde{X}^6\Delta_i$ FeNC. For CoCN, the quoted uncertainty for $r_0(\text{C-N})$ is $\sigma = 0.0010$ Å and again, the 1σ -interval does not overlap with the 1.16–1.19 Å interval, even though the uncertainty on r_0 is much smaller than for ${}^6\Delta_i$ FeNC.

FeNC and CoCN are not the only two molecules for which ‘too-short’ experimentally derived values of $r_0(\text{C-N})$ have been reported. For ${}^2\Delta_{i,\Omega=5/2}$ NiCN, $r_0(\text{C-N}) = 1.1591(29)$ [9] and 1.1590(2) Å [10], for ${}^1\Sigma^+$ CuCN [11], $r_0(\text{C-N}) = 1.1576(1)$ Å, and for ${}^2\Sigma^+$ ZnCN [12], $r_0(\text{C-N}) = 1.1464$ Å. In all instances, the numbers in parentheses are quoted uncertainties in units of the last digit given. Nor is the problem restricted to molecules containing first-row transition metal atoms. Recent reports have added $\tilde{X}^2\Pi$ BrCN⁺ [13] ($r_0 = 1.103(78)$ Å), $\tilde{X}^6\Sigma^+$ CrCN [14] ($r_0 = 1.1529(12)$ Å, $r_m^{(1)} = 1.148$ Å), ${}^1\Sigma^+$ AgCN [15] ($r_0 = 1.15527(67)$ Å, $r_m^{(2)} = 1.160259(58)$ Å), and ${}^1\Sigma^+$ AuCN [15] ($r_0 = 1.1586(24)$ Å, $r_s = 1.158654(10)$ Å) to the list.

A conventional method to derive an ‘experimental’ structure for linear triatomic cyanides and isocyanides has been to determine the B_0 values for at least two isotopologues and assume that these values are consistent with the same rigid linear structure defined in terms of two internuclear distances. The experimental B_0 values then deliver at least two equations which can be solved (possibly in a least-squares sense) to produce ‘ r_0 ’ values, which are customarily interpreted as vibrationally averaged bond lengths. As demonstrated recently for FeNC [1] (and discussed already in 1967 for CsOH, and later for RbOH, by Lide and co-workers [16–18] and in modern times by Watson *et al.* [19] in general terms and by Walker *et al.* [20] in work on cyanides and isocyanides of Al, Ga, and In), the r_0 values determined by this procedure lack physical meaning if the molecule exhibits large-amplitude bending motion.

For CoCN, we have studied the ground and low-lying excited electronic states theoretically [21]. We have calculated *ab initio* two-dimensional potential energy surfaces, expressed in terms of the Co-C and C-N internuclear distances, for these states at the MR-SDCI+Q+ E_{rel} /[Roos ANO (Co), aug-cc-pVQZ(C,N)] level of theory [21] (the notation will be explained in Section 2 below). The ground electronic state has been confirmed to be ${}^3\Phi$, in agreement with the experimental findings by Sheridan *et al.* [8]. We computed the equilibrium bond lengths to be 1.8540 Å for the Co-C bond and 1.1677 Å for the C-N bond; these values differ significantly from the experimental r_0 -values derived by Sheridan *et al.* [8] from their rotational spectra. In Ref. [21], we further reported vertical excitation energies of various electronic states of the triplet, quintet, and singlet manifolds, and we proposed a new spin-orbit coupling scheme quite different from that suggested by Sheridan *et al.* [8].

In the present work, we have extended the study of Ref. [21] to determine the three-dimensional potential energy surfaces (PES’s) for $\tilde{X}^3\Phi_i$ CoCN at the *ab initio* level of theory of MR-SDCI+Q+ E_{rel} /[Roos ANO (Co), aug-cc-pVQZ (C, N)] also employed in Ref. [21]. Special care has been taken to account for the quasi-degeneracy of nearby low-lying electronic states as well as the constraint due to the C_s symmetry. Although the electronic state $\tilde{X}^3\Phi$ CoCN is in principle Renner-degenerate, the degeneracy has been found to be negligibly small, so that we have employed the ${}^6A'$ PES, which is indistinguishable from the ${}^6A''$ PES to within 0.005 cm^{-1} at the molecular geometries considered in the *ab initio* calculation, for the subsequent calculations of ro-vibrational parameters and energies. We derived molecular constants from the *ab initio* PES by the second-order perturbation method [22–24] and the MORBID [4–7] variational method. Comparing the expectation values of the internuclear distances r obtained from MORBID wavefunctions with experimentally derived r_0 values, we conclude that the effect of large amplitude bending motion should explicitly be taken into account when r_0 values are calculated from observed B_0 values.

2 THE *AB INITIO* CALCULATIONS

The molecule $\tilde{X}^3\Phi$ CoCN can be represented approximately as $\text{Co}^{\delta+}(\text{CN})^{\delta-}$, so that it has a basically ionic Co-C bond. This is confirmed by the Mulliken populations that we obtain as +0.893 for Co, -0.789 for C, and -0.104 for N at the MR-SDCI/[Wachters + *f* (Co), aug-cc-pVTZ (C, N)] level of theory (see below for the definition of method and basis set). Hence, the degenerate character of the wavefunctions of Co^+ should be retained more or less in the CoCN molecule as a quasi-degeneracy. Thus, we need to exert special care to describe correctly the quasi-degeneracy under the C_s symmetry constraint. Since the electronic state $\tilde{X}^3\Phi$ CoCN cannot be described by a single configuration state function (CSF) [21], we must do multi-reference calculations. In order to account for the non-dynamical (i.e. static) and dynamical electron correlation, we carried out multi-reference singles and doubles configuration interaction (MR-SDCI) molecular orbital calculations. To include dynamical electron correlations from the quadruple excitation CSF's and to recover part of the size-consistency, the Davidson correction [25], denoted as Q, was added to the energies obtained from the MR-SDCI calculations. If spectroscopic accuracy is to be achieved, relativistic corrections are known to be necessary [1, 26, 27] even for first-row transition metal radicals. Therefore, the MR-SDCI+Q energy has been corrected for relativistic effects by the Cowan-Griffin perturbation method [28], i.e., by computing expectation values E_{rel} of the mass-velocity and one-electron Darwin terms. Thus, the *ab initio* method employed in the present work will be denoted as MR-SDCI+Q+ E_{rel} .

All molecular orbital calculations have been performed with the MOLPRO 2002.6 [29] suite of quantum chemistry programs. Roos' ANO basis set, (21*s*,15*p*,10*d*,6*f*,4*g*)/[8*s*,7*p*,5*d*,3*f*,2*g*] [30], was employed for Co, and Dunning's aug-cc-pVQZ basis sets, (13*s*,7*p*,4*d*,3*f*,2*g*)/[6*s*,5*p*,4*d*,3*f*,2*g*] [31, 32], for C and N. The set of basis sets will be denoted as [Roos ANO (Co), aug-cc-pVQZ (C, N)]. For the calculation of the spin-orbit interaction constant A_{SO} and the Mulliken population, a Wachters + *f* basis set, (14*s*,11*p*,6*d*,3*f*)/[8*s*,6*p*,4*d*,1*f*] [33–35], was used for Co, and Dunning's aug-cc-pVTZ basis sets, (11*s*,6*p*,3*d*,2*f*)/[5*s*,4*p*,3*d*, 2*f*] [31, 32], for C and N. This combination will be denoted as [Wachters + *f* (Co), aug-cc-pVTZ (C, N)].

The actual procedure for the MR-SDCI+Q+ E_{rel} energy calculation at geometries of C_s symmetry is as follows. In order to ensure the quasi-degeneracy under the C_s symmetry constraints, the initial-guess orbitals for the state averaged complete active space self consistent field (SA-CASSCF) calculation were constructed by merging the SA-CASSCF orbitals of Co^+ in C_s symmetry (corresponding to the dissociation limit $3d^8\ ^3F$ electronic ground state of Co^+ [36]) with the $^1A'$ SA-CASSCF orbitals of CN^- (corresponding to the $^1\Sigma^+$ orbitals in C_{2v} symmetry) at the geometry with equilibrium bond lengths (which we know from Ref. [21]) and the Co-C-N bond angle of 178° . These guessed orbitals were optimized at the level of [3-4]-SA-CASSCF with closed occupation restriction for the orbitals originating in the Co 1*s*, 2*s*, 2*p*, 3*s*, 3*p*, and the C and N 1*s* orbitals. The notation [3-4] denotes the state-average of three A' and four A'' states, done under the C_s symmetry constraint. That is, full-valence, no-core SA-CASSCF (with 18 electrons distributed over 14 orbitals) has been carried out to include non-dynamical electron correlation. The resultant SA-CASSCF natural orbitals (NO's) are checked in terms of energy, character, and l_z^2 values with the SA-CASSCF NO's calculated under the C_{2v} symmetry constraint (i.e., CASSCF NO's averaged over $A_1\ \Delta$, $B_1\ \Phi$ and Π , $B_2\ \Phi$ and Π , and $A_2\ \Sigma$ and Δ states in C_{2v} symmetry). Starting with these guessed orbitals, the [3-4]-SA-CASSCF orbitals for other geometries with the Co-C-N bond angle of 178° and given Co-C bond length (1.804-1.887 Å) and C-N bond length (1.098-1.248 Å) were calculated by the same method. The [3-4]-SA-CASSCF orbitals for the Co-C-N bond angles of 175, 170, 163, and 154° were calculated successively, using the NO's at the previous angle (starting from the NO's at 178°) as the initial guess in order to maintain the correct orbital character which should be correlated to that of the NO's at the linear geometry.

Based on the [3-4]-SA-CASSCF orbitals, internally contracted MR-SDCI calculations have been carried out for the two C_s symmetry species A' and A'' , respectively, with the active space consisting of 10*a'*-18*a'* and 3*a''*-6*a''* orbitals, i.e., orbitals originating in Co 3*d* and 4*s* orbitals and in C and N 2*s* and 2*p* orbitals. The highest *a'* valence orbital 19*a'* was excluded due to the CPU-time cost on our computers. Thus, these MR-SDCI calculations involve 18 electrons distributed over 13 orbitals. The C_s symmetry constraint has been taken into account in the MR-SDCI calculations by including an A'' reference space

in the A' MR-SDCI calculations, and A' reference space for A'' calculations, respectively. The expansion of the wavefunctions was truncated to disregard the configurations with MR-SDCI coefficients below 0.01. Thus, the number of CSF's in the reference space of the MR-SDCI calculations generated from the active space is 117054 for the $A' {}^3\Phi$ state, for example, and the corresponding dimension of the internally contracted (uncontracted) CI matrix reaches 9.2×10^7 (3.0×10^{10}). The energies and dipole moments thus obtained were interpolated and extrapolated, respectively, to the Co-C-N angle of 180° . Davidson's correction Q and the Cowan-Griffin relativistic correction E_{rel} were added to the MR-SDCI energies. The Mulliken population was calculated at the MR-SDCI/[Wachters + f (Co), aug-cc-pVTZ (C, N)] level of theory, and the spin-orbit coupling constant was calculated at the same level of theory with the Breit-Pauli operator [37] applied to the MR-SDCI wavefunctions.

The three-dimensional potential energy surface was constructed from the MR-SDCI+ Q + E_{rel} energies calculated in C_s symmetry for 180 unique geometries. In total, 330 geometries were considered. The electronic energies computed at these geometries were fitted to a polynomial expansion

$$V(r_{12}, r_{32}, \theta) = \sum_{j=0}^4 \sum_{k=0}^4 \sum_{l=0,2,4,6} \frac{1}{j!k!l!} f_{jkl} \Delta r_{12}^j \Delta r_{32}^k (\theta - \theta_e)^l \quad (1)$$

in internal displacement coordinates. The bond length displacements in equation (1) are given as $\Delta r_{i2} = r_{i2} - r_{i2}^e$, $i = 1$ or 3 . Here, r_{12} is the instantaneous value of the Co-C distance in Å (the Co nucleus is labeled 1 and the C nucleus is labeled 2) and r_{32} is the instantaneous value of the C-N distance in Å (N is labeled 3). The bond angle $\theta = \angle(\text{Co-C-N})$ is given in radian; its equilibrium value is $\theta_e = \pi$. The optimized equilibrium bond lengths are $r_{12}^e = r_e(\text{Co-C}) = 1.8540$ Å and $r_{32}^e = r_e(\text{C-N}) = 1.1677$ Å, and the energy value at equilibrium is $E_e = f_{000} = -1484.759198 E_h$. The optimized values of the other force constants f_{jkl} are listed in table 1. The maximum and root-mean-square errors achieved in the fitting were 2.06 and 0.43 cm^{-1} , respectively.

3 SPECTROSCOPIC PARAMETERS CALCULATED BY PERTURBATION METHODS

To derive the standard spectroscopic constants by perturbation methods [22–24], we have expanded the PES in terms of Simons-Parr-Finlan coordinates $Q_i = 1 - r_{i2}^{(\text{ref})}/r_{i2}$, $i = 1$ or 3 , for the bond lengths defined above, and the bending coordinate $Q_2 = \theta - \theta^{(\text{ref})}$ (measured in radian). Here, $r_{i2}^{(\text{ref})} = r_{i2}^e$, $i = 1$ or 3 , and $\theta^{(\text{ref})} = \pi$ radian. The three-dimensional PES calculated at the MR-SDCI+ Q + E_{rel} /[Roos ANO (Co), aug-cc-pVQZ (C, N)] level of theory was fitted to an expansion in these coordinates:

$$V(Q_1, Q_2, Q_3) = \sum_{j=0}^4 \sum_{k=0,2,4,6} \sum_{l=0}^4 C_{jkl} Q_1^j Q_2^k Q_3^l. \quad (2)$$

The optimized values of the expansion coefficients C_{jkl} in equation (2) are available from the authors on request. The optimized equilibrium-structure parameters are $r_{12}^{(\text{ref})} = r_e(\text{Co-C}) = 1.8540$ Å and $r_{32}^{(\text{ref})} = r_e(\text{C-N}) = 1.1677$ Å; these values are identical to those obtained in the displacement coordinate fitting (equation (1)). Based on the the fitted polynomial potential energy function in equation (2), standard spectroscopic constants such as B_0 , D_J , α_i , ω_i , x_{ij} , ... for Co^{12}CN and Co^{13}CN have been computed from perturbation expressions [22–24]. The values obtained are given in table 2, together with the available experimental counterparts. The spin-orbit coupling constant A_{SO} and dipole moment μ , which were derived directly from *ab initio* molecular orbital calculations, are also included.

In table 2 we note the discrepancy of 3.2% between, on one hand, the *ab initio* value of $r_e(\text{C-N})$ and, on the other hand, the experimentally derived value of $r_0(\text{C-N})$. We feel that this discrepancy is too large to be explained by the fact that we are comparing r_e and r_0 . As a numerical experiment, we have tried to generate ' $r_{0,\Omega=4}$ ' bond length values from the theoretically predicted rotational constants $B_{0,\Omega=4}$

Table 1. Force constants f_{jkl} (equation (1)) for $^3A'$ CoCN obtained from the computed *ab initio* energies.

$f_{200}/\text{aJ } \text{\AA}^{-2}$	3.23251485	$f_{230}/\text{aJ } \text{\AA}^{-5}$	989.44515584
$f_{110}/\text{aJ } \text{\AA}^{-2}$	0.15704300	$f_{140}/\text{aJ } \text{\AA}^{-5}$	-2361.95889439
$f_{020}/\text{aJ } \text{\AA}^{-2}$	17.45618091	$f_{302}/\text{aJ } \text{\AA}^{-3}$	93.84987495
f_{002}/aJ	0.15279289	$f_{212}/\text{aJ } \text{\AA}^{-3}$	-15.65301999
$f_{300}/\text{aJ } \text{\AA}^{-3}$	0.47303865	$f_{122}/\text{aJ } \text{\AA}^{-3}$	1.17549762
$f_{210}/\text{aJ } \text{\AA}^{-3}$	-2.08713939	$f_{032}/\text{aJ } \text{\AA}^{-3}$	-3.60631090
$f_{120}/\text{aJ } \text{\AA}^{-3}$	0.67173991	$f_{104}/\text{aJ } \text{\AA}^{-1}$	0.96532247
$f_{030}/\text{aJ } \text{\AA}^{-3}$	-116.91961733	$f_{014}/\text{aJ } \text{\AA}^{-1}$	-0.20642941
$f_{102}/\text{aJ } \text{\AA}^{-1}$	0.06980685	$f_{420}/\text{aJ } \text{\AA}^{-6}$	-2507.56169154
$f_{012}/\text{aJ } \text{\AA}^{-1}$	-0.29956404	$f_{330}/\text{aJ } \text{\AA}^{-6}$	-4113.69774958
$f_{400}/\text{aJ } \text{\AA}^{-4}$	438.58551596	$f_{240}/\text{aJ } \text{\AA}^{-6}$	5100.63047033
$f_{310}/\text{aJ } \text{\AA}^{-4}$	-23.41673003	$f_{402}/\text{aJ } \text{\AA}^{-4}$	4455.52601768
$f_{220}/\text{aJ } \text{\AA}^{-4}$	-23.59246531	$f_{312}/\text{aJ } \text{\AA}^{-4}$	-85.64660751
$f_{130}/\text{aJ } \text{\AA}^{-4}$	-2.13469295	$f_{222}/\text{aJ } \text{\AA}^{-4}$	582.10500427
$f_{040}/\text{aJ } \text{\AA}^{-4}$	591.27472492	$f_{132}/\text{aJ } \text{\AA}^{-4}$	468.61980982
$f_{202}/\text{aJ } \text{\AA}^{-2}$	0.62305853	$f_{042}/\text{aJ } \text{\AA}^{-4}$	716.10366608
$f_{112}/\text{aJ } \text{\AA}^{-2}$	-0.54701771	$f_{204}/\text{aJ } \text{\AA}^{-2}$	32.29205396
$f_{022}/\text{aJ } \text{\AA}^{-2}$	-0.43446090	$f_{114}/\text{aJ } \text{\AA}^{-2}$	4.88143433
f_{004}/aJ	-0.20313302	$f_{024}/\text{aJ } \text{\AA}^{-2}$	16.52080969
$f_{410}/\text{aJ } \text{\AA}^{-5}$	4629.44952826	f_{006}/aJ	-7.25567748
$f_{320}/\text{aJ } \text{\AA}^{-5}$	-2153.98551015		

for Co^{12}CN and Co^{13}CN , assuming a linear structure for CoCN. This calculation gives $r_{0,\Omega=4}(\text{Co-C}) = 1.8604 \text{ \AA}$ and $r_{0,\Omega=4}(\text{C-N}) = 1.1503 \text{ \AA}$. The C-N distance obtained in this manner is substantially different from the r_0 value of $1.1313(10) \text{ \AA}$ reported in Ref. [8]. This means that the r_0 bond lengths are very sensitive to the combination of B_0 values used to determine them. However, unlike the case of FeNC [2], the pure rotational spectroscopic measurements made for CoCN [8] produce highly accurate values of $B_{0,\Omega=4}$ and so here, the ‘too-short’ C-N r_0 values cannot be blamed on lack of accuracy of the experimentally derived B_0 values. We note that the deviations between the theoretically predicted and experimentally determined values of $B_{0,\Omega=4}$ (table 2) are 0.48 and 0.70 %, respectively, for Co^{12}CN and Co^{13}CN . Thus, we conclude that, as in the case of FeNC [2], the source of the discrepancy between $r_e(\text{C-N})$ and $r_0(\text{C-N})$ is associated with the determination of $r_0(\text{C-N})$ from the experimental B_0 (or $B_{0,\Omega=4}$) values: In this determination, the large-amplitude bending motion is not accounted for.

There is another notable contradiction in table 2: The theoretically predicted value for the spin-orbit interaction parameter A_{SO} of $\tilde{X}^3\Phi_i$ CoCN is -242 cm^{-1} whereas Sheridan *et al.* [8] assumed a value of -133 cm^{-1} from the experimentally derived values for $X^3\Phi_i$ CoCl (-166 cm^{-1} [38]) and $X^3\Phi_i$ CoH (-221.5 cm^{-1} [39]; this value calculated from the observed $\Omega = 4-3$ spin-splitting of $-728(3) \text{ cm}^{-1}$ determined by Varberg *et al.* [40] by laser excitation spectroscopy). Our value is close to $A_{\text{SO}} = -232.9 \text{ cm}^{-1}$ determined experimentally for $X^3\Phi_i$ CoF by Adam and Hamilton [41].

We calculate the harmonic vibrational wavenumber for the Co-C stretching mode, ω_3 , to be 544 cm^{-1} from the three-dimensional *ab initio* PES. This value is somewhat different from the estimated experimental value of $\sim 478 \text{ cm}^{-1}$ [8]. We expect that in the near future, this vibrational energy can be directly measured by rotation-vibration spectroscopy. The bending harmonic vibrational wavenumber ω_2 is as low as 239

Table 2. Standard spectroscopic constants for Co¹²CN and Co¹³CN in the ³Φ_i ground electronic state.^a

	Co ¹² CN		Co ¹³ CN	
	Present work ^b	Exp. [8] ^c	Present work ^b	Exp. [8] ^c
$r_e(\text{Co-C})/\text{\AA}$	1.8540	1.8827(7) ^d	1.8540	
$r_e(\text{C-N})/\text{\AA}$	1.1677	1.1313(10) ^d	1.1677	
$\angle_e(\text{Co-C-N})/\text{deg}$	180		180	
B_e/MHz	4210.5		4169.3	
B_0/MHz	4230.7	4208.827(23)	4188.5	
$B_{0,\Omega=4}/\text{MHz}$	4229.1	4200.653(31)	4186.9	4157.68(31)
D_J/MHz	0.00108	0.001451(10)	0.00107	
α_1/cm^{-1}	0.00042		0.00040	
α_2/cm^{-1}	−0.00083		−0.00078	
α_3/cm^{-1}	−0.00011		−0.00011	
q_2/cm^{-1}	0.000180		0.000182	
ζ_{12}	−0.976		−0.975	
ζ_{23}	−0.216		−0.222	
ω_1/cm^{-1}	2191		2142	
ω_2/cm^{-1}	239		232	
ω_3/cm^{-1}	544	~ 478	537	
x_{11}/cm^{-1}	−12.3		−11.8	
x_{22}/cm^{-1}	−8.4		−6.7	
x_{33}/cm^{-1}	−0.7		−0.7	
x_{12}/cm^{-1}	−3.8		−3.6	
x_{13}/cm^{-1}	−2.7		−2.5	
x_{23}/cm^{-1}	35.3		27.9	
g_{22}/cm^{-1}	8.4		6.6	
ν_1^e/cm^{-1}	2162		2113	
ν_2^e/cm^{-1}	238		231	
ν_3^e/cm^{-1}	576		563	
ZPVE/ cm^{-1}	1609		1573	
$A_{\text{so}}^f/\text{cm}^{-1}$	−242	−133 ^g	−242	
μ_e^h/D	−6.992 (−7.482)		−6.992 (−7.482)	

^a r_e , \angle_e , B_e : equilibrium bond length, bond angle, and rotational constant, respectively. B_0 : rotational constant in the vibrational ground state. D_J : centrifugal distortion constant. α_i : rotation-vibration interaction constant. q_2 : ℓ -doubling constant. ζ_{ij} : Coriolis coupling constant. ω_i : harmonic vibrational wavenumber. x_{ij} , g_{22} : anharmonic vibrational constants. ZPVE: the zero-point vibrational energy.

^bParameters obtained from the *ab initio* data at the MR-SDCI+Q+ E_{rel} /[Roos ANO (Co), aug-cc-pVQZ (C, N)] level of theory, as described in Section 2.

^cNumbers in parentheses are quoted uncertainties in units of the last digit given.

^d r_0 value determined from the values of $B_{0,\Omega=4}$ for Co¹²CN and Co¹³CN.

^eVibrational term values calculated from the ω_i , x_{ij} , and g_{22} parameter values.

^fSpin-orbit coupling constant calculated at the MR-SDCI/[Wachters+ f (Co), aug-cc-pVTZ (C, N)] level of theory.

^gAssumed value (see text).

^hDipole moment value at the equilibrium structure, calculated as finite electric field derivative of the MR-SDCI+Q+ E_{rel} energy. The value in parentheses is the corresponding expectation value.

cm^{-1} . This value reflects the shallow bending potential and is consistent with the small values of the bending force constants in table 1: The bending motion has large amplitude.

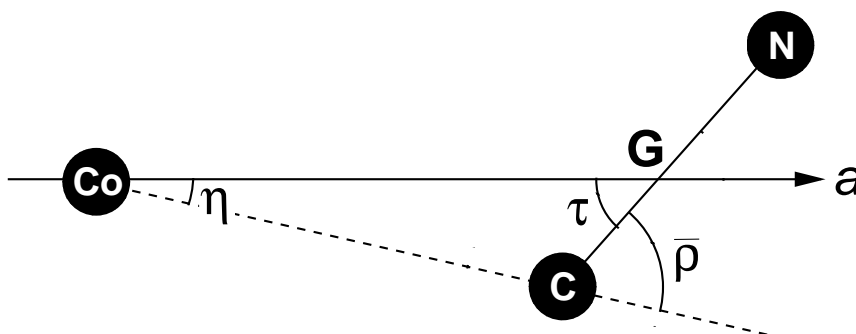


Figure 1. The definitions of the angles $\bar{\rho}$, τ , and η used to describe the geometry of the CoCN molecule. The axis labeled 'a' passes through the Co nucleus and through G, the center of mass of the CN moiety.

4 THE MORBID CALCULATION

4.1 The potential energy surface

In table 2, we have reported values of the customary spectroscopic parameters B_0 , D_J , α_i , ω_i , x_{ij} , ...; these values are obtained from perturbation-theory expressions: Anharmonic terms and rotation-vibration interaction terms in the rotation-vibration Hamiltonian are considered as perturbations of a harmonically vibrating, rigidly rotating molecule. Perturbation-theory treatments are usually successful for the lower rovibrational excited states when no strong Fermi resonances are present in the molecule studied.

Since the bending potential is shallow as shown by the bending force constants in table 1, large amplitude bending motion may limit the accuracy of the perturbation treatment. Thus, we carry out variational calculations for CoCN by means of the MORBID (Morse Oscillator Rigid Bender Internal Dynamics) program [4–7].

For this analysis, we adopted three Jacobi-type coordinates to describe the geometry of CoCN: The C-N distance $r_{\text{C-N}}$, the Co-G distance $R_{\text{Co-G}}$, and the angle $\tau = \angle(\text{Co-G-C})$, where G is the center of mass of the CN fragment; see figure 1.

As a first step towards doing MORBID calculations, we fit an analytical representation of the potential energy surface through the *ab initio* points for CoCN; the analytical expression is chosen as

$$V(\Delta r_{12}, \Delta r_{32}, \bar{\rho}) = \sum_{jkl} G_{jkl} y_1^j y_3^k (1 - \cos \bar{\rho})^l \quad (3)$$

with

$$y_i = 1 - \exp(-a_i[r_{i2} - r_{i2}^e]). \quad (4)$$

The quantity y_i in equation (4) is expressed in terms of the molecular constants a_i and the instantaneous internuclear distance values r_{i2} , $i = 1$ or 3 (see equation (1) and the discussion following it). The quantity $\bar{\rho} = \pi - \theta$ (where θ is the bond angle as defined above), and the G_{jkl} are expansion coefficients. The function y_1 in equation (3) pertains to the Co-C bond, whereas y_3 pertains to the C-N bond.

From the computed *ab initio* energies we have determined the expansion coefficients G_{jkl} in equation (3), and the parameters a_i and r_{i2}^e in equation (4) by least-squares fitting to the *ab initio* energies. In the final fitting to 180 points we could usefully vary 14 parameters. We had to constrain $a_1 = 2.0 \text{ \AA}^{-1}$ and $a_3 = 2.5 \text{ \AA}^{-1}$, and G_{003} was constrained to 20000 cm^{-1} in order to ensure that the potential energy function have no spurious secondary minima at large values of $\bar{\rho}$. As in the case of FeNC [1] we could get the best fit to the *ab initio* energies by constraining the equilibrium bond lengths to the values determined when equation (1) was fitted through the *ab initio* points. The standard deviation of the final fitting to determine the G_{jkl} values was 1.5 cm^{-1} . The optimized parameter values are given in table 3.

Table 3. The potential energy parameters of $^3A'$ CoCN obtained by fitting the analytical function of equation (3) through the calculated *ab initio* energies.^a

$r_{12}^e/\text{\AA}$	1.8540 ^{b,c}	G_{101}	2501.9(830) ^d
$r_{32}^e/\text{\AA}$	1.1677 ^c	G_{020}	70178.8(353)
$a_1/\text{\AA}^{-1}$	2.0	G_{200}	20572.9(202)
$a_3/\text{\AA}^{-1}$	2.5	G_{110}	1552.6(672)
G_{000}/E_h^e	-1484.7591948(11)	G_{111}	-3537.1(14668)
G_{001}	7771.9(127)	G_{030}	7966.1(708)
G_{002}	-3740.7(1236)	G_{300}	22621.1(15030)
G_{003}	20000	G_{210}	-5472.0(13216)
G_{011}	-6256.9(352)	G_{040}	4230.9(11204)
		G_{400}	78796.5(294570)

^aUnits are cm^{-1} unless otherwise indicated. The parameters r_{12}^e and a_1 pertain to the Co-C bond, whereas r_{32}^e and a_3 pertain to the C-N bond. The expansion coefficients G_{jkl} are defined in equation (3).

^bParameters, for which no standard error is given, were held fixed in the least squares fit.

^cDetermined in preliminary least squares fittings.

^dQuantities in parentheses are standard errors in units of the last digit given.

^e G_{000} is the potential energy value at equilibrium.

4.2 Rotation-vibration energies and structural parameters

MORBID calculations of the rotation-vibration energies for Co^{12}CN and Co^{13}CN have been carried out with the following basis set (see Ref. [4]): The stretching problem was prediagonalized with Morse oscillator functions $|n_1n_3\rangle$ having $n_1 + n_3 \leq N_{\text{Stretch}} = 12$. In constructing the final rotation-vibration matrices we used the $N_{\text{Bend}} = 12$ lowest bending basis functions and the $N_A = 15$ lowest stretching basis functions of A' symmetry in the molecular symmetry group $\mathbf{C}_s(\text{M})$ [42].

In table 4, we list calculated vibrational energy spacings for Co^{12}CN and Co^{13}CN , calculated with the MORBID program from the potential energy parameters from table 3. We include in the table also the term values calculated by perturbation methods (i.e., from the rotation-vibration parameters ω_i , x_{ij} , g_{22} , B_0 , α_i , D_J , ... given in table 2; see Refs. [22–24]).

There are rather large discrepancies between the MORBID energies and those calculated by perturbation methods, in particular for excited bending states. The bending term values calculated by perturbation theory show a much stronger anharmonicity than those calculated with MORBID. For example, the ratio $E(0, 7^1, 0)/E(0, 1^1, 0)$ is 6.4 for the MORBID results and 5.3 for the PT results. The very pronounced anharmonicity of the PT results are due to the fact that two anharmonic constants, $x_{23} \approx 35 \text{ cm}^{-1}$ and $g_{22} \approx 8 \text{ cm}^{-1}$, are unusually large for Co^{12}CN and Co^{13}CN . We attribute this to the fact that the harmonic vibrational wavenumber ω_3 is fairly close to $2\omega_2$, and that this gives rise to resonant (i.e., small) energy denominators in the second-order-perturbation-theory expressions for x_{23} and g_{22} . In the MORBID calculations, no perturbation theory is used and the problem of resonant denominators is therefore circumvented. In view of this, we expect the MORBID results in table 4 to be more accurate than the PT ones.

Effective rotational constants B_{eff} for Co^{12}CN and Co^{13}CN are given in table 5. These B_{eff} -values are derived from term values calculated with the MORBID program from the potential energy parameters in table 3.

We also compute vibrationally averaged structural parameters as expectation values in terms of the rovibrational wavefunctions obtained in the MORBID calculation. To define the structural parameters, we use the angles η , τ , and $\bar{\rho}$ introduced in figure 1 together with the a axis which passes through the Co nucleus and center of mass G of the CN moiety (so that it also passes through the nuclear center of mass). Since the Co nucleus is much heavier than the C and N nuclei combined this axis is close, but not

Table 4. The vibrational energy spacings $E(v_1, v_2^{\ell_2}, v_3, N_{\min} = \ell_2) - E(0, 0^0, 0, 0)$ for $^3A'$ Co¹²CN and Co¹³CN (in cm⁻¹).

$(v_1, v_2^{\ell_2}, v_3)$	N_{\min}	Co ¹² CN		Co ¹³ CN	
		MORBID ^a	PT ^b	MORBID ^a	PT ^b
(0,0 ⁰ , 0)	0	0.00 ^c	0.0	0.00 ^d	0.0
(0,1 ^{1e,f} , 0)	1	237.78	237.6	230.69	230.6
(0,2 ⁰ , 0)	0	460.74	441.1	448.33	434.4
(0,2 ^{2e,f} , 0)	2	473.92	475.0	459.98	461.2
(0,3 ^{1e,f} , 0)	1	675.10	644.9	658.49	638.3
(0,3 ^{3e,f} , 0)	3	711.26		689.29	
(0,4 ⁰ , 0)	0	895.88	814.8	873.79	815.3
(0,4 ^{2e,f} , 0)	2	899.85	848.7	877.49	842.1
(0,4 ^{4e,f} , 0)	4	946.78		919.0	
(0,5 ^{1e,f} , 0)	1	1098.23	984.8	1072.97	992.5
(0,6 ⁰ , 0)	0	1318.89	1120.8	1287.96	1142.8
(0,7 ^{1e,f} , 0)	1	1515.19	1257.0	1481.46	1293.3
(0,0 ⁰ , 1)	0	586.17	576.0	577.80	562.7
(0,1 ^{1e,f} , 1)	1	850.59	848.8	831.43	821.2
(0,2 ⁰ , 1)	0	1079.40	1087.6	1054.25	1052.9
(0,2 ^{2e,f} , 1)	2	1100.44	1121.5	1072.92	1079.7
(1,0 ⁰ , 0)	0	2175.32	2161.7	2125.31	2113.1
(1,1 ^{1e,f} , 0)	1	2406.80	2395.4	2349.48	2340.2
(1,2 ⁰ , 0)	0	2629.51	2595.2	2567.39	2540.4
(1,2 ^{2e,f} , 0)	2	2639.13	2629.1	2575.88	2567.2

^aCalculated using the MORBID program with the potential energy parameters from table 3.

^bCalculated with Perturbation Theory, i.e., from the rotation-vibration parameters ω_i , x_{ij} , g_{22} , B_0 , α_i , D_J , ... given in table 2 (see Refs. [22–24]).

^cThe zero point energy is 1608.84 cm⁻¹.

^dThe zero point energy is 1573.78 cm⁻¹.

identical, to the a principal axis [42] of the molecule. The projections of the Co-C distance r_{12} and the C-N distance r_{32} onto the a axis are $r_{12} \cos \eta$ and $r_{32} \cos \tau$, respectively, and in table 6 we give averaged values of these quantities for the states with $(v_1, v_2^{\ell_2}, v_3, N = \ell_2) = (0, 0^0, 0, 0)$, $(0, 1^{1e,f}, 0, 1)$, $(0, 2^0, 0, 0)$, $(1, 0^0, 0, 0)$, and $(0, 0^0, 1, 0)$ of Co¹²CN and Co¹³CN. The table also gives averaged values of r_{12} , r_{32} , and $\bar{\rho}$ (see figure 1 for definition).

It should be noted that the $\langle r_{12} \rangle$ and $\langle r_{32} \rangle$ values in table 6 are slightly longer than the corresponding r_e values in table 2 of 1.8540 and 1.1677 Å, respectively, and that each value remains approximately constant (at about 1.873 and 1.172 Å, respectively) as long as the corresponding stretching motion is not excited. Thus, the bond lengths determined as the MORBID expectation values should be regarded as physically sound, proper bond lengths characterizing the nature of the associated chemical bonds.

The expectation values $\langle r_{12} \cos \eta \rangle$ and $\langle r_{32} \cos \tau \rangle$ in table 6 are computed in an approximation where $\cos \tau$ and $\cos \eta$ are obtained as functions of $\bar{\rho}$ in the reference configuration [4], where the bond lengths are held fixed at their equilibrium values, $r_{12} = r_{12}^e$ and $r_{32} = r_{32}^e$. The expectation values $\langle r_{12} \rangle$, $\langle r_{32} \rangle$, $\langle r_{12} \cos \eta \rangle$, and $\langle r_{32} \cos \tau \rangle$ are calculated with the ‘fully coupled’ wavefunctions given in equation (10) of

Table 5. Effective rotational constants B_{eff} (in MHz) for $^3A'$ Co 12 CN and Co 13 CN, derived from term values calculated with the MORBID program using the potential energy parameters in table 3.

$(v_1, v_2^{\ell_2}, v_3)$	Co 12 CN	Co 13 CN
$(0, 0^0, 0)$	4236.967 ^a	4194.396
$(0, 1^{1e}, 0)$	4251.057	4207.887
$(0, 1^{1f}, 0)$	4256.453	4213.283
$(0, 2^0, 0)$	4286.732	4241.763
$(0, 2^{2e,f}, 0)$	4279.537	4235.168
$(0, 3^{1e}, 0)$	4293.328	4248.959
$(0, 3^{1f}, 0)$	4303.521	4259.151
$(0, 3^{3e,f}, 0)$	4305.619	4259.751
$(0, 4^0, 0)$	4332.601	4286.433
$(0, 4^{2e,f}, 0)$	4323.307	4278.038
$(0, 4^{4e,f}, 0)$	4331.401	4284.334
$(0, 0^0, 1)$	4224.076	4181.805
$(0, 1^{1e}, 1)$	4243.562	4200.092
$(0, 1^{1f}, 1)$	4249.558	4205.788
$(0, 2^0, 1)$	4275.040	4230.671
$(0, 2^{2e,f}, 1)$	4272.043	4226.774
$(1, 0^0, 0)$	4230.371	4190.499
$(1, 1^{1e}, 0)$	4234.868	4192.598
$(1, 1^{1f}, 0)$	4239.965	4197.694
$(1, 2^0, 0)$	4272.642	4230.671
$(1, 2^{2e,f}, 0)$	4263.648	4219.879

^aThe experimental value is 4208.827(23) MHz [8]; quoted uncertainty in parentheses.

Ref. [6], whereas in order to calculate $\langle \bar{\rho} \rangle$ and its quantum-mechanical uncertainty $\delta \bar{\rho}$, we define

$$\langle \bar{\rho}^n \rangle = \int_0^\pi \bar{\rho}^n \left| \Psi_{\text{bend}}^{(v_2, \ell_2)} \right|^2 d\bar{\rho}, \tag{5}$$

where $n = 1$ or 2 , and $\Psi_{\text{bend}}^{(v_2, \ell_2)}$ is the normalized bending basis wavefunction with the largest contribution to the vibrational state in question. We now have $\delta \bar{\rho} = \sqrt{\langle \bar{\rho}^2 \rangle - \langle \bar{\rho} \rangle^2}$. We note that for all states considered, $\langle \bar{\rho} \rangle$ is significantly larger than $\delta \bar{\rho}$.

As expected, table 6 also shows that the C-N bond length projected onto the a -axis, $\langle r_{32} \cos \tau \rangle$, becomes shorter as the bending motion is excited. The quantity $\langle \bar{\rho} \rangle$ keeps a constant value of $8(5)^\circ$ unless the bending mode is excited, and increases with the bending-vibration quantum number. Although the equilibrium structure is linear, the ro-vibrationally averaged structure is bent as much as $8(5)^\circ$ (where the quantity is parentheses is the quantum mechanical uncertainty) out of linearity even at the zero-point structure. This displacement angle is a little smaller than the value for FeNC of $13(7)^\circ$ [1], reflecting that the bending motion of CoCN is a little ‘tighter’ than that of FeNC, even though the bending potential of CoCN is shallow as shown in figure 2.

Now we have reliable, theoretically-derived r_0 bond lengths which can be directly compared to the experimentally derived r_0 value. Since the theoretically predicted and experimentally observed values of $B_{0, \Omega=4}$, 4229.1 and 4200.653(31) MHz, respectively, differ by only 0.48%, the difference in theoretically

Table 6. Expectation values (in Å unless otherwise indicated) of geometrical parameters^a (see text) for ³A' Co¹²CN and Co¹³CN, calculated with MORBID wavefunctions generated from the potential energy parameters in table 3.

	$(v_1, v_2^{\ell_2}, v_3)$	$\langle r_{12} \rangle$	$\langle r_{32} \rangle$	$\langle r_{12} \cos \eta \rangle$	$\langle r_{32} \cos \tau \rangle$	$\langle \bar{\rho} \rangle / \text{deg}$
Co ¹² CN	(0,0 ⁰ , 0)	1.8733	1.1718	1.8701	1.1608	8(5) ^b
	(0,1 ^{1e,f} ,0)	1.8772	1.1727	1.8735	1.1524	13(5)
	(0,2 ⁰ , 0)	1.8732	1.1727	1.8665	1.1413	15(8)
	(1,0 ⁰ , 0)	1.8740	1.1796	1.8702	1.1644	8(5)
	(0,0 ⁰ , 1)	1.8819	1.1720	1.8786	1.1612	8(5)
Co ¹³ CN	(0,0 ⁰ , 0)	1.8730	1.1718	1.8699	1.1609	9(5)
	(0,1 ^{1e,f} ,0)	1.8765	1.1727	1.8731	1.1526	13(5)
	(0,2 ⁰ , 0)	1.8727	1.1727	1.8663	1.1415	16(8)
	(1,0 ⁰ , 0)	1.8734	1.1794	1.8695	1.1629	9(5)
	(0,0 ⁰ , 1)	1.8812	1.1720	1.8781	1.1613	9(5)

^a r_{12} is the Co-C distance, and r_{32} is the C-N distance.

^bQuantities in parentheses are quantum-mechanical uncertainties $\delta \bar{\rho}$ (see text) in units of degrees.

predicted (1.1718 Å) and experimentally derived (1.1313(10) Å) $r_0(\text{C-N})$ values (which amounts to 3.5%) indicates that the conventional quasi-linear approach employed in deriving r_0 values from the observed values of B_0 for different isotopologues is inadequate for CoCN. As in the case of ⁶Δ_i FeNC [1], we conclude that the short, experimentally derived $r_0(\text{C-N})$ value for CoCN is caused by the neglect of its large amplitude bending motion in the calculation of r_0 .

4.3 Dipole moment surfaces

Following Ref. [6] we calculate the dipole moment components in an xqp axis system taken to be right-handed with origin in the nuclear center of mass. The x axis is perpendicular to the molecular plane, and the p axis is parallel to the Co-C bond. The p and q axes are directed so that for CoCN the q coordinate of the N nucleus and the p coordinate of the Co nucleus are both positive.

The nonvanishing dipole moment functions are $\bar{\mu}_q = \langle \Psi_{\text{elec}} | \mu_q | \Psi_{\text{elec}} \rangle_{\text{el}}$ and $\bar{\mu}_p = \langle \Psi_{\text{elec}} | \mu_p | \Psi_{\text{elec}} \rangle_{\text{el}}$, where Ψ_{elec} is the electronic wavefunction of ³A' CoCN and the subscript 'el' indicates that integration is over the electronic coordinates only. These electronic matrix elements are expressed as parameterized functions of the nuclear coordinates, where the parameter values are obtained by fitting to our *ab initio* values of the molecular dipole moments. For $\bar{\mu}_q$ and $\bar{\mu}_p$ we use the following analytical functions of the vibrational coordinates:

$$\bar{\mu}_q(\Delta r_{12}, \Delta r_{32}, \bar{\rho}) = \sin \bar{\rho} \sum_{jkl} \mu_{jkl}^{(q)} \Delta r_{12}^j \Delta r_{32}^k (1 - \cos \bar{\rho})^l \quad (6)$$

and

$$\bar{\mu}_p(\Delta r_{12}, \Delta r_{32}, \bar{\rho}) = \sum_{jkl} \mu_{jkl}^{(p)} \Delta r_{12}^j \Delta r_{32}^k (1 - \cos \bar{\rho})^l \quad (7)$$

where $\mu_{jkl}^{(q)}$ and $\mu_{jkl}^{(p)}$ are expansion coefficients.

The values of $\bar{\mu}_q$ and $\bar{\mu}_p$ were obtained *ab initio* at the 180 geometries where the potential energy surface

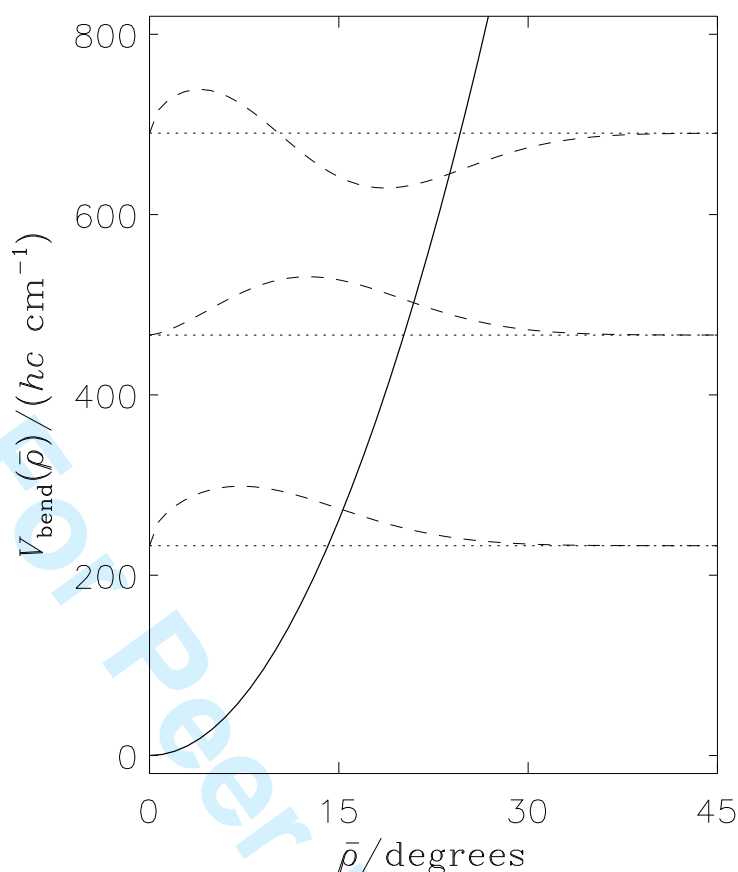


Figure 2. The bending potential energy function of CoCN (solid curve), plotted as a function of $\bar{\rho} = \pi - \angle(\text{Co-C-N})$. The bond lengths are held fixed at their equilibrium values. The lowest three bending vibrational energies with $v_2^{\ell_2} = 0^0, 1^1$, and 2^0 , respectively, are indicated by dotted lines and for each energy, the corresponding bending wavefunction (consistent with the volume element $d\bar{\rho}$) is drawn as a dashed curve. All three wavefunctions are drawn on the same arbitrary ordinate scale. The energies and wavefunctions indicated in the figure are obtained in a rigid-bender calculation (i.e., they are calculated under the assumption that the molecule bends with the bond lengths fixed at their equilibrium values). The three energies (given relative to an energy zero at the potential minimum) are 232.7, 466.4, and 690.3 cm^{-1} , respectively.

was determined. The calculated values have been fitted to the analytical expressions in equations (6)–(7). The fittings of $\bar{\mu}_p$ and $\bar{\mu}_q$ had standard deviations of 0.00059 and 0.00005 D, respectively. The parameter values obtained are given in table 7.

4.4 Transition moments and intensities

We have used the computer program described in Ref. [6] for simulating selected rotation-vibration bands of $^3A'$ CoCN using as input the potential energy parameters from table 3 and the electric dipole moment parameters from table 7.

In table 8 we report vibrational transition moments for Co^{12}CN . The transition moments obtained for Co^{13}CN are so similar to the Co^{12}CN results that we do not list them.

A practical difficulty with simulating spectra of molecules as heavy as CoCN is the fact that owing to the small rotational constants of approximately 0.14 cm^{-1} , very highly excited rotational states will be populated in molecules at room-temperature thermal equilibrium. In order to obtain simulations that resemble realistic spectra (i.e., simulations in which the P and R branches do not end abruptly at an N value determined by computer limitations), we have chosen to calculate integrated absorption coefficients at $T = 12 \text{ K}$. The results of the simulations are given in figures 3–7. The figures show the integrated absorption coefficients for rovibrational transitions involving $N \leq 20$ and line strength $S(f \leftarrow i) \geq 0.001 \text{ D}^2$ for the rotational spectra (figure 3), the ν_2 fundamental bands (figure 4), the $2\nu_2$ bands (figure 5), and the ν_3

Table 7. The electric dipole moment parameters of CoCN obtained by fitting the analytical functions of equations (6)–(7) through the calculated *ab initio* values.

	$\mu^{(p)}$	$\mu^{(q)}$
μ_{000}/D	7.481720(91) ^{a,b}	−1.429850(77)
μ_{001}/D	−1.709(15)	0.2491(31)
μ_{002}/D	1.64(49)	−0.350(24)
μ_{003}/D	−6.81(35)	
$\mu_{100}/\text{D } \text{\AA}^{-1}$	5.346(31)	−0.9931(22)
$\mu_{010}/\text{D } \text{\AA}^{-1}$	0.8502(28)	−0.7752(12)
$\mu_{101}/\text{D } \text{\AA}^{-1}$	−0.498(67)	−0.067(27)
$\mu_{011}/\text{D } \text{\AA}^{-1}$	−0.582(35)	−1.260(14)
$\mu_{110}/\text{D } \text{\AA}^{-2}$	0.91(13)	−1.257(39)
$\mu_{200}/\text{D } \text{\AA}^{-2}$	4.213(90)	
$\mu_{020}/\text{D } \text{\AA}^{-2}$	−2.476(31)	0.598(11)
$\mu_{030}/\text{D } \text{\AA}^{-3}$	1.90(71)	

^aQuantities in parentheses are standard errors in units of the last digit given.

^b $\mu_{000}^{(p)}$ is the electric dipole moment at equilibrium.

Table 8. Vibrational transition moments M_{vib} for Co¹²CN (in D).^a

	(0, 0 ⁰ , 0)	(0, 1 ¹ , 0)	(0, 2 ⁰ , 0)	(0, 2 ² , 0)	(0, 3 ¹ , 0)	(0, 3 ³ , 0)	(0, 4 ⁰ , 0)	(0, 4 ² , 0)	(0, 4 ⁴ , 0)
(0, 0 ⁰ , 0)	7.469								
(0, 1 ¹ , 0)	0.157	7.445							
(0, 2 ⁰ , 0)	0.023	−0.158	7.423						
(0, 2 ² , 0)		0.003		7.422					
(0, 3 ¹ , 0)	0.002	0.032	0.223	−0.158	7.400				
(0, 3 ³ , 0)				0.273		7.400			
(0, 4 ⁰ , 0)	0.001	−0.002	0.044		−0.223		7.378		
(0, 4 ² , 0)				0.038	0.273	−0.159		7.378	
(0, 4 ⁴ , 0)						0.316			7.377
	(1, 0 ⁰ , 0)	(1, 1 ¹ , 0)	(0, 0 ⁰ , 1)	(0, 1 ¹ , 1)					
(0, 0 ⁰ , 0)	−0.079	0.005	−0.203	−0.011					
(0, 1 ¹ , 0)	0.005	−0.079	−0.011	−0.200					
(0, 2 ⁰ , 0)		−0.004	−0.003	0.001					
(0, 2 ² , 0)				−0.014					

^aTransition moments with $\Delta\ell = 0$ are matrix elements $\langle v'_1, (v'_2)^\ell, v'_3 | \mu_z | v''_1, (v''_2)^\ell, v''_3 \rangle$ and transition moments with $|\Delta\ell| = 1$ are matrix elements $\langle v'_1, (v'_2)^{\ell\pm 1}, v'_3 | \mu_y | v''_1, (v''_2)^\ell, v''_3 \rangle$. Only transition moments with absolute values $|M_{\text{vib}}| \geq 0.001$ D are listed.

and ν_1 fundamental bands (figures 6 and 7). In all calculations, we neglect the splittings resulting from the non-zero electron spin and from the Renner effect. In all cases, we simulate spectra of Co¹²CN and Co¹³CN with the C isotopes in their natural abundances (98.9% for ¹²C and 1.1% for ¹³C). However, in practice, the Co¹³CN lines are so weak relative to the Co¹²CN ones that they are hardly discernible in the figures. The weak band at the low-wavenumber end of figure 7 is not the ν_1 band of Co¹³CN. It is the $10\nu_2^0$ band of Co¹²CN which is obviously very weak intrinsically, but which borrows intensity from the ν_1 band.

We do not give here detailed tables of the transition wavenumbers, line strengths, and lower state energies of individual transitions in the bands simulated in figures 3-7. Such listings are available from the authors on request. However, for CoCN, the transition wavenumbers and lower state energies can be estimated to

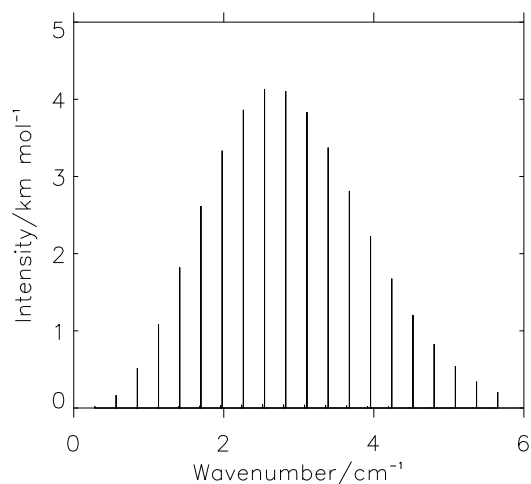


Figure 3. The rotational spectra of Co¹²CN and Co¹³CN with the C isotopes in their natural abundances simulated *ab initio* at $T = 12$ K.

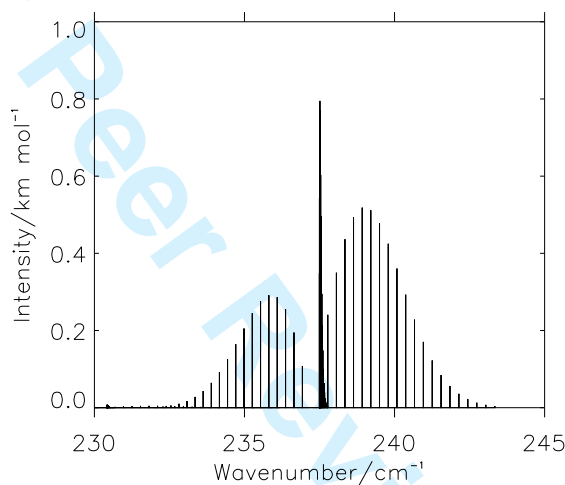


Figure 4. The ν_2 fundamental bands of Co¹²CN and Co¹³CN with the C isotopes in their natural abundances simulated *ab initio* at $T = 12$ K.

high accuracy from the vibrational energy spacings in table 4 in conjunction with the expression for the rotational energy

$$E_{\text{rot}}(N) = B_{\text{eff}}N(N + 1) \tag{8}$$

where values for the effective rotational constant B_{eff} are given in tables 5. Values for the strengths of individual lines can be estimated from the vibrational transition moments M_{vib} given in table 8. By inserting the vibrational transition moment values in equation (12.31) of Ref. [43], approximate values of the line strengths of individual rotation-vibration can be computed. These line strength values can then be inserted in equation (1.9) of Ref. [43] together with values of $E_{\text{rot}}(N)$ from equation (8), and integrated absorption coefficients can be estimated.

5 SUMMARY AND CONCLUSION

We have constructed *ab initio* potential energy surfaces and dipole moment surfaces for CoCN in its electronic ground state $\tilde{X}^3\Phi_i$ at the MR-SDCI+Q+ E_{rel} /[Roos ANO (Co), aug-cc-pVQZ (C, N)] level of theory. Using the potential energy functions, we have obtained values of the standard spectroscopic

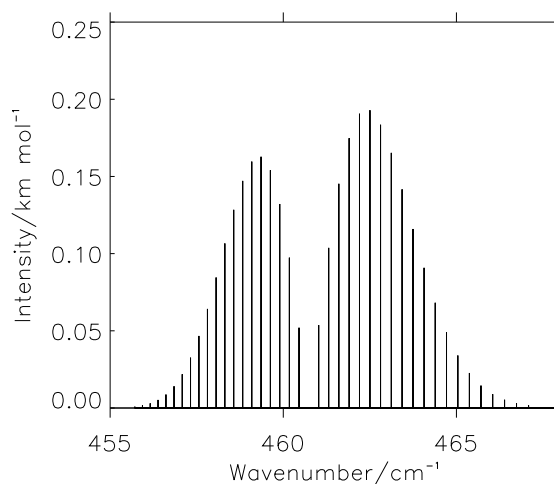


Figure 5. The $2\nu_2$ bands of Co^{12}CN and Co^{13}CN with the C isotopes in their natural abundances simulated *ab initio* at $T = 12$ K.

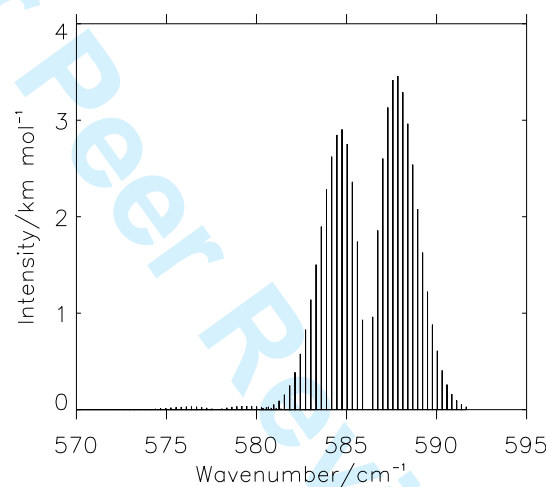


Figure 6. The ν_3 bands of Co^{12}CN and Co^{13}CN with the C isotopes in their natural abundances simulated *ab initio* at $T = 12$ K.

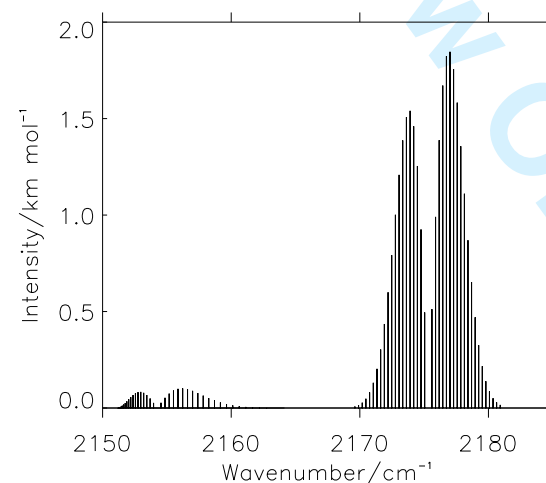


Figure 7. The ν_1 bands of Co^{12}CN and Co^{13}CN with the C isotopes in their natural abundances simulated *ab initio* at $T = 12$ K. The weak band around 2154 cm^{-1} is the $10\nu_2^0$ band of Co^{12}CN .

parameters by perturbation methods, and we have solved the rotation-vibration Schrödinger equation variationally by means of the MORBID program. The rotation-vibration wavefunctions from MORBID were used to compute ro-vibrationally averaged structural parameters in the lowest rotation-vibration states of CoCN. Also, we have used the potential energy surfaces and the dipole moment surfaces to obtain vibrational transition moments for selected vibrational transitions, and we have simulated the rotational spectrum for some rotation-vibration bands. We neglect the extremely small Renner splittings in the $\tilde{X}^3\Phi_i$ state of CoCN.

One important aim of the present work is to provide theoretical predictions which hopefully will facilitate further experimental studies of CoCN, in particular of its vibrational transitions. Another aim, however, is the precise determination of the structure of the molecule. To determine a traditional ' r_0 ' (or, in the present case, an ' $r_{0,\Omega=4}$ ') structure, Sheridan *et al.* [8] have used the values of the rotational constant $B_{0,\Omega=4}$ obtained from rotational spectra for Co¹²CN and Co¹³CN. Their calculation yields the value 1.1313 Å, with a quoted uncertainty of $\sigma = 0.0010$ Å, for the C-N bond length. As pointed out above, even generous confidence intervals around the value of 1.1313 Å do not overlap with the interval of 1.16-1.19 Å where we typically expect to find C-N bond lengths. The reason for the abnormally short, experimentally derived C-N bond length of CoCN is the same as we have discussed at length for FeNC in Ref. [1]: In the determination of the 'experimental' bond length, the bending motion is neglected in that the molecular structure is assumed to be linear. This is a poor approximation for $\tilde{X}^3\Phi_i$ CoCN where, even though the equilibrium structure is linear, the rovibrationally averaged, ground-state structure is bent with $\langle\bar{\rho}\rangle = 180^\circ - \langle\angle(\text{Co-C-N})\rangle = 8(5)^\circ$ (the quantity in parentheses is the quantum mechanical uncertainty). It is an even worse approximation for $\tilde{X}^6\Delta_i$ FeNC, where the corresponding averaged angle is $13(7)^\circ$ [1].

So, for $\tilde{X}^3\Phi_i$ CoCN we conclude, by analogy with the conclusions reached for $\tilde{X}^6\Delta_i$ FeNC in Ref. [1], that the r_0 (or $r_{0,\Omega=4}$) structure determined in the traditional manner from the analysis of experimental spectra has little physical meaning. It is natural to ask whether there is an alternative method for determining the structure, which could be easily implemented by experimental spectroscopists and which would be capable of extracting correct structural information from experimentally determined parameter values. For molecules such as CoCN and FeNC [1], for which only the lowest vibronic states of two isotopologues have been experimentally characterized, no such method exists. However, when several excited bending states have also been characterized for two isotopologues one can, for example, follow Lide and Kuczkowski [16], who measured the B values of CsOH and CsOD in several excited bending states. With the measured values, they could make an extrapolation to find the B value of a hypothetical 'bending-less' state which has the stretching vibrations in their ground states. From the extrapolated, bending-less B values, they obtained very reasonable bond lengths, whereas the traditional method produced a 'suspiciously short' OH bond length.

If an *ab initio* potential energy surface (or at least a potential energy curve for the bending motion) is available for the molecule in question, experimental information can be used to refine this surface in least-squares fittings with, for example, a rigid-bender model for describing the bending motion. Such fittings yield reliable structural information which, however, is not solely derived from experiment but also from the *ab initio* potential surface/curve. Examples of this approach, which is not easily implemented by experimental spectroscopists, are afforded by the work of Walker *et al.* [20] on cyanides and isocyanides of Al, Ga, and In, and by the work by Bunker, Jensen and co-workers (see Refs. [44,45] and references therein) on \tilde{X}^3B_1 CH₂.

In order to obtain reliable structural information as done by Lide and Kuczkowski [16], it is necessary to observe molecular transitions involving several excited bending states. In many cases this is not possible. In the typical situation where only vibronic ground states can be spectroscopically characterized, it would appear that for small molecules such as CoCN and FeNC, the most reliable structural information can be obtained in *ab initio* calculations such as those reported for CoCN in the present work and for FeNC in Ref. [1], possibly followed by a refinement in least-squares fittings to the experimental data as described in Refs. [20,44,45].

1
2
3
4
5
6
7
8
9
10
11
12
13
14
15
16
17
18
19
20
21
22
23
24
25
26
27
28
29
30
31
32
33
34
35
36
37
38
39
40
41
42
43
44
45
46
47
48
49
50
51
52
53
54
55
56
57
58
59
60

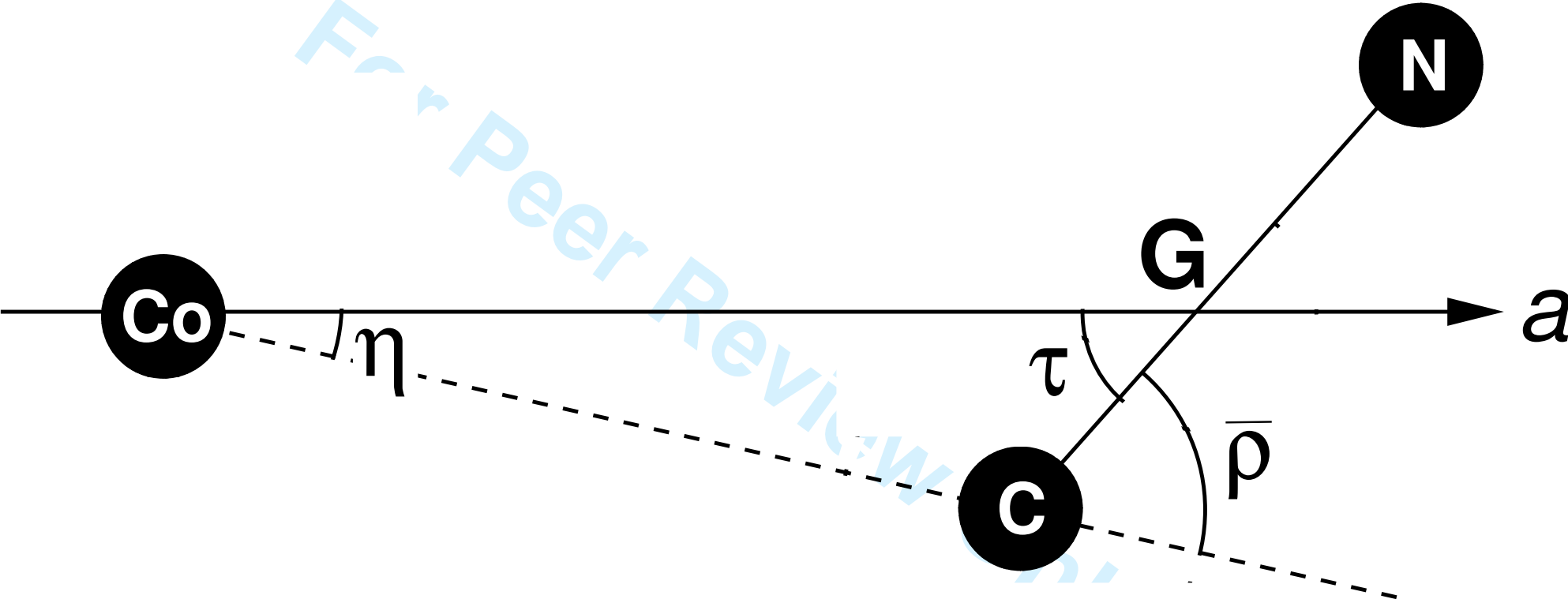
ACKNOWLEDGMENTS

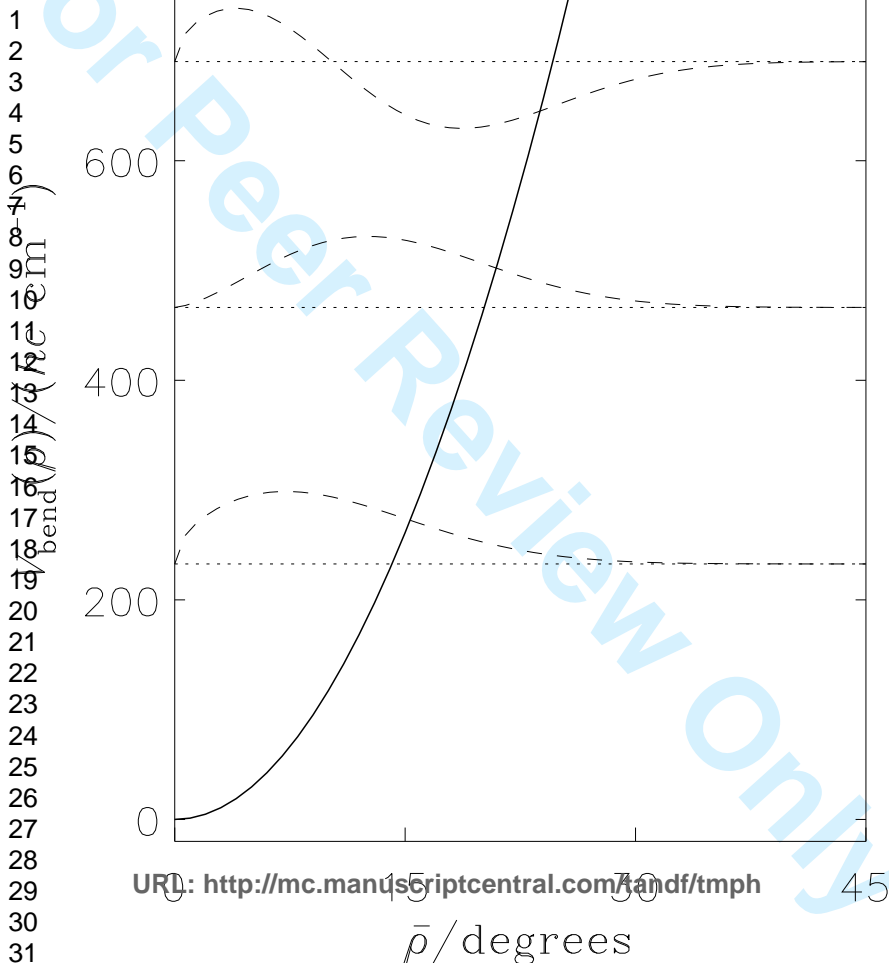
We thank P. M. Sheridan and L. M. Ziurys for providing us with their experimental CoCN data prior to publication. The methods for *ab initio* MO calculations employed in the present work to treat CoCN, such as the selection of the active space, the basis sets, and the construction of adequate SA-CASSCF orbitals, have been developed by Yukari Mitsui, Michiko Amano, and Sachiko S. Itono during their thesis studies at Ochanomizu University. The work of T. H., R. O., and U. N. is supported in part by the program CREST (Core Research for Evolutional Science and Technology), Japan. The work of P. J. is supported in part by the Deutsche Forschungsgemeinschaft and the Fonds der Chemischen Industrie.

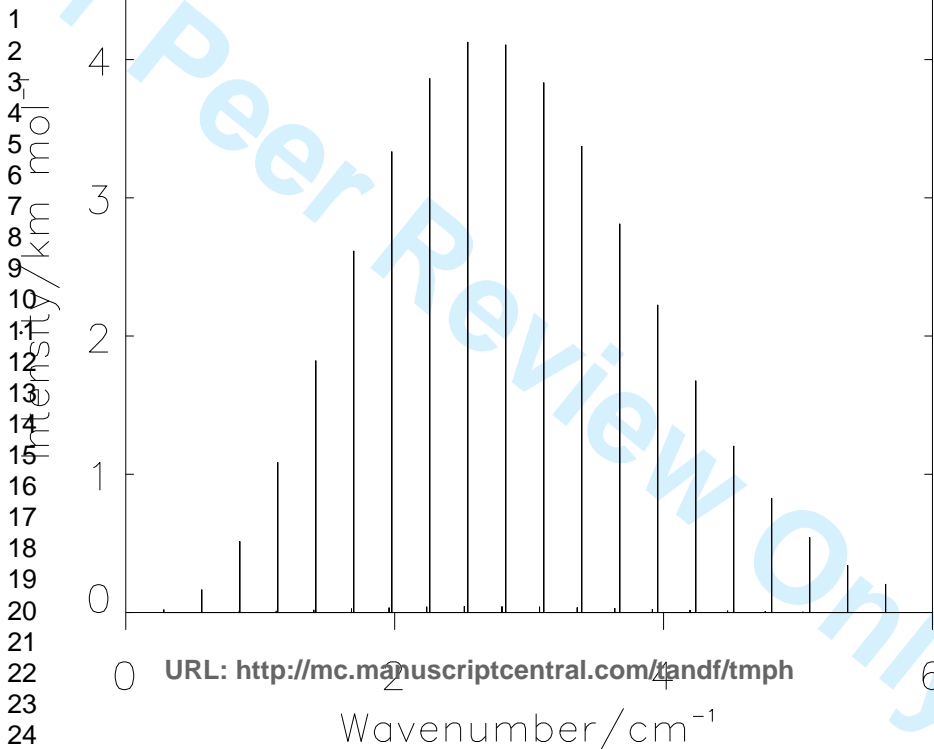
For Peer Review Only

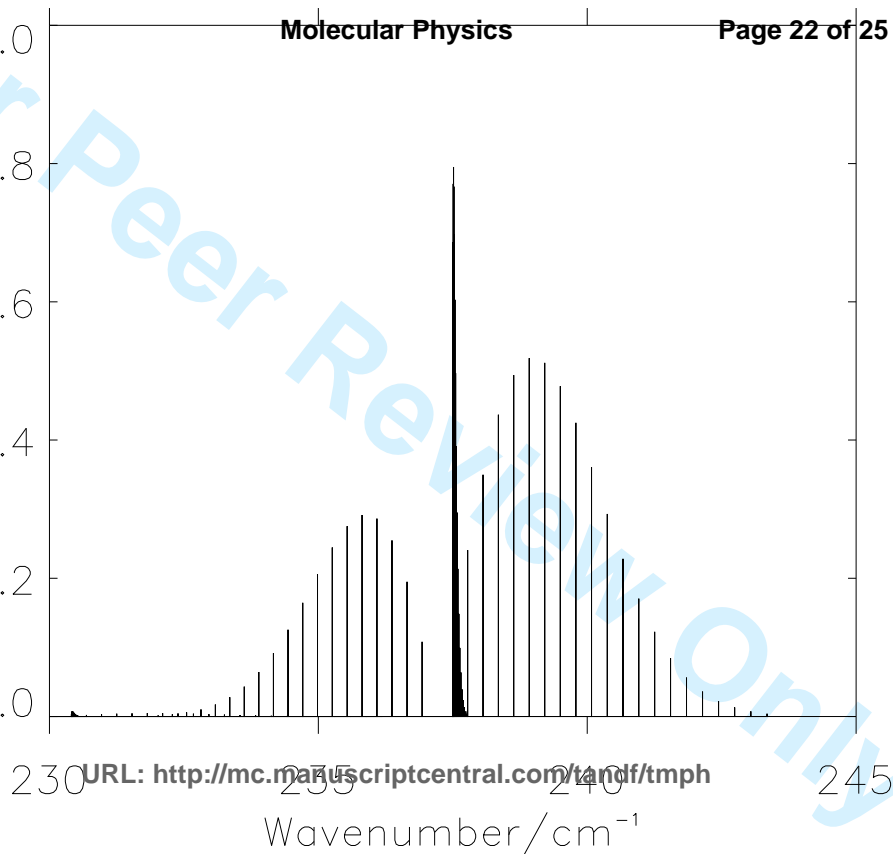
References

- [1] T. Hirano, R. Okuda, U. Nagashima, V. Špirko, and P. Jensen. *J. Mol. Spectrosc.*, **236**, 234 (2006).
- [2] J. Lie and P. J. Dagdigian. *J. Chem. Phys.*, **114**, 2137 (2001).
- [3] N. J. DeYonker, Y. Yamaguchi, W. D. Allen, C. Pak, H. F. Schaefer III, and K. A. Peterson. *J. Chem. Phys.*, **120**, 4726 (2004).
- [4] P. Jensen. *J. Mol. Spectrosc.*, **128**, 478 (1988).
- [5] P. Jensen. *J. Chem. Soc., Faraday Trans. 2*, **84**, 1315 (1988).
- [6] P. Jensen. *J. Mol. Spectrosc.*, **132**, 429 (1988).
- [7] P. Jensen. In *Methods in Computational Molecular Physics*, S. Wilson and G. H. F. Diercksen, (Eds), Plenum Press, New York, NY (1992).
- [8] P. M. Sheridan, M. A. Flory, and L. M. Ziurys. *J. Chem. Phys.*, **121**, 8360 (2004).
- [9] C. T. Kingston, A. J. Merer, and T. D. Varberg. *J. Mol. Spectrosc.*, **215**, 106 (2002).
- [10] P. M. Sheridan and L. M. Ziurys. *J. Chem. Phys.*, **118**, 6370 (2003).
- [11] D. B. Grotjahn, M. A. Brewster, and L. M. Ziurys. *J. Am. Chem. Soc.*, **124**, 5895 (2002).
- [12] M. A. Brewster and L. M. Ziurys. *J. Chem. Phys.*, **117**, 4853 (2002).
- [13] Y. Nakashima, T. Ogawa, M. Matsuo, and K. Tanaka. Paper MG12 presented at the 60th Ohio State University International Symposium on Molecular Spectroscopy, Columbus, OH (2005).
- [14] M. A. Flory and L. M. Ziurys. Paper TH04 presented at the 61st Ohio State University International Symposium on Molecular Spectroscopy, Columbus, OH (2006).
- [15] E. Y. Okabayashi, T. Okabayashi, F. Koto and M. Tanimoto. Paper RE09 presented at the 61st Ohio State University International Symposium on Molecular Spectroscopy, Columbus, OH (2006).
- [16] D. R. Lide, Jr., and R. L. Kuczkowski. *J. Chem. Phys.*, **46**, 4768 (1967).
- [17] C. Matsumura and D. R. Lide, Jr.. *J. Chem. Phys.*, **50**, 71 (1969).
- [18] D. R. Lide, Jr., and C. Matsumura. *J. Chem. Phys.*, **50**, 3080 (1969).
- [19] J. K. G. Watson, A. Roytburg, and W. Ulrich. *J. Mol. Spectrosc.*, **196**, 102 (1999).
- [20] K. A. Walker, C. J. Evans, S.-H. K. Suh, M. C. L. Gerry, and J. K. G. Watson. *J. Mol. Spectrosc.*, **209**, 178 (2001).
- [21] R. Okuda, U. Nagashima, P. Jensen, and T. Hirano. *Chem. Phys. Letters*, submitted for publication.
- [22] I. M. Mills. In *Molecular Spectroscopy, Modern Research, Vol. 1*, K. Narahari Rao and C. W. Mathews (Eds), Academic Press, New York, NY (1972).
- [23] A. R. Hoy, I. M. Mills, and G. Strey. *Mol. Phys.*, **24**, 1265 (1972).
- [24] K. Sarka and J. Demaison. In *Computational Molecular Spectroscopy*, P. Jensen and P. R. Bunker (Eds), Wiley, Chichester, UK (2000).
- [25] S. R. Langhoff and E. R. Davidson. *Int. J. Quantum Chem.*, **8**, 61 (1974).
- [26] J. F. Harrison. *Chem. Rev.*, **100**, 679 (2000).
- [27] S. S. Itono, T. Taketsugu, T. Hirano, and U. Nagashima. *J. Chem. Phys.*, **115**, 11213 (2001).
- [28] R. D. Cowan and D. C. Griffin. *J. Opt. Soc. Am.*, **66**, 1010 (1976).
- [29] MOLPRO, version 2002.6, is a package of *ab initio* programs designed by H.-J. Werner and P. J. Knowles. It is based on previous versions by R. D. Amos, A. Bernhardsson, A. Berning, P. Celani, D. L. Cooper, M. J. O. Deegan, A. J. Dobbyn, F. Eckert, C. Hampel, G. Hetzer, P. J. Knowles, T. Korona, R. Lindh, A.W. Lloyd, S. J. McNicholas, F. R. Manby, W. Meyer, M. E. Mura, A. Nicklass, P. Palmieri, R. Pitzer, G. Rauhut, M. Schütz, U. Schumann, H. Stoll, A. J. Stone, R. Tarroni, T. Thorsteinsson, and H.-J. Werner.
- [30] R. Pou-Amérigo, M. Merchán, I. Nebot-Gil, P.-O. Widmark, and B. O. Roos. *Theor. Chim. Acta*, **92**, 149 (1995).
- [31] T. H. Dunning, Jr.. *J. Chem. Phys.*, **90**, 1007 (1989).
- [32] R. A. Kendall, T. H. Dunning, Jr., and R. J. Harrison. *J. Chem. Phys.*, **96**, 6796 (1992).
- [33] C. W. Bauschlicher, Jr., S. R. Langhoff, H. Partridge, and L. A. Barnes. *J. Chem. Phys.*, **91**, 2399 (1989). A Wachters +*f* basis set from the EMSL Basis Set Library (<http://www.emsl.pnl.gov/forms/basisform.html>) was employed.
- [34] A. J. H. Wachters. *J. Chem. Phys.*, **52**, 1033 (1970).
- [35] P. J. Hay. *J. Chem. Phys.*, **66**, 4377 (1977).
- [36] NIST Atomic Spectra Database Levels Form, http://physics.nist.gov/PhysRefData/ASD/levels_form.html
- [37] A. Berning, M. Schweizer, H. -J. Werner, P. J. Knowles, and P. Palmieri. *Mol. Phys.*, **98**, 1823 (2000).
- [38] M. A. Flory, D. T. Halfen, and L. M. Ziurys. *J. Chem. Phys.*, **121**, 8385 (2004).
- [39] S. P. Beaton, K. M. Evenson, and J. M. Brown. *J. Mol. Spectrosc.*, **164**, 395 (1994).
- [40] T. D. Varberg, E. J. Hill, and R. W. Field. *J. Mol. Spectrosc.*, **138**, 630 (1989).
- [41] A. G. Adam and W. D. Hamilton. *J. Mol. Spectrosc.*, **206**, 139 (2001).
- [42] P. R. Bunker and P. Jensen. *Molecular Symmetry and Spectroscopy*, 2nd Edition, NRC Research Press, Ottawa, Canada (1998).
- [43] P. R. Bunker and P. Jensen. *Fundamentals of Molecular Symmetry*, IOP Publishing, Bristol, UK (2004).
- [44] P. R. Bunker. *Ann. Rev. Phys. Chem.*, **34**, 59 (1983).
- [45] P. Jensen and P. R. Bunker. *J. Chem. Phys.*, **89**, 1327 (1988).

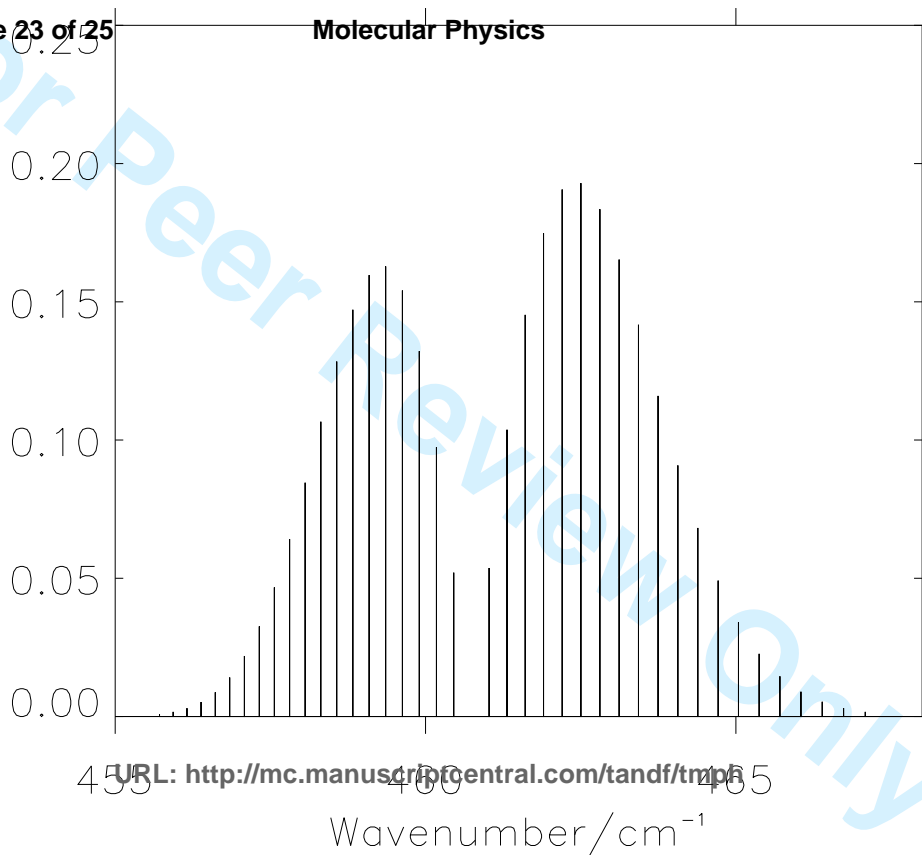








1
2
3
4
5
6
7
8
9
10
11
12
13
14
15
16
17
18
19
20
21
22
23
24
25



1
2
3
4
5
6
7
8
9
10
11
12
13
14
15
16
17
18
19
20
21
22
23
24
25

